sustainability

MDPI

Article

Development and Life Cycle Assessment of High-Volume Biomass Ash-Based Hybrid Alkaline Cements for Low-Carbon Green Cement

Xuan Cui [1], Luchang Xiong [1,2,*], Olga Maltseva [2], Zhijun Wan [1] and Angel Palomo [2]

[1] School of Mines, China University of Mining and Technology, Xuzhou 221116, China; xcui@cumt.edu.cn (X.C.); zhjwan@cumt.edu.cn (Z.W.)
[2] Instituto de Ciencias de la Construcción Eduardo Torroja (IETcc-CSIC), 28033 Madrid, Spain; olgamaltseva@ietcc.csic.es (O.M.); palomo@ietcc.csic.es (A.P.)
* Correspondence: lchxiong@cumt.edu.cn

Abstract

The cement industry accounts for about 8% of global CO_2 emissions, and alkali-activated materials with high solid waste content can help achieve decarbonization of the cement industry and sustainable development, offering promising technical pathways for the development of low-carbon green cement. Biomass ash, as a promising raw material for solid-waste valorization, is limited due to its low substitution rate and poor early strength. This study determined the optimal pretreatment method for high-content (≥70%) biomass-ash-based blended cement and prepared biomass-ash-based hybrid alkaline cements (BHACs) with the aid of chemical additives. The 28 d compressive strength of the ground-ash-based blended cement reached 34.59 MPa. Single-component sodium sulfate achieved the highest 2 d strength (38.4 MPa), whereas sodium citrate reduced early strength. The synergistic effect of binary mixtures was limited, whereas sodium sulfate–sodium citrate combinations have the potential to achieve a balance between strength and flowability. Life cycle assessment (LCA) shows that, compared with CEM I 52.5R, all citrate-free BHAC groups reduce global warming potential (GWP) by over 59.42% and cumulative energy demand (CED) by over 45.67%. Based on early compressive strength and a "cradle to gate" life cycle assessment, BHACs are considered to have the potential to balance mechanical and environmental performance, promoting the industrial-scale solid-waste valorization of biomass ash for green low-carbon construction materials.

Keywords: biomass ash; mechanochemical activation; hybrid alkaline cement; low-clinker cement; life cycle assessment; low-carbon green cement

Check for updates

Academic Editor: Igor Palčić

Received: 2 October 2026
Revised: 27 October 2026
Accepted: 28 October 2026
Published: 31 October 2026

Copyright: © 2026 by the authors. Licensee MDPI, Basel, Switzerland. This article is an open access article distributed under the terms and conditions of the Creative Commons Attribution (CC BY) license.

1. Introduction

Cement is one of the irreplaceable basic materials in modern infrastructure construction. Its huge production scale has made it one of the main sources of greenhouse gas emissions in the global industrial sector. Currently, annual global cement production exceeds 4 billion tons [1], and it is expected to further increase to over 5 billion tons in the coming decades with the continuous development of urbanization and infrastructure construction [2]. Meanwhile, cement production contributes approximately 8% of global CO_2 emissions [1,3], with the primary emissions stemming from the decarbonization reaction of limestone during the cement production process and the combustion of fossil fuels [4]. Therefore, in the context of global carbon neutrality, reducing the demand for cement

production and decreasing carbon emissions per unit of cement are crucial avenues for promoting deep decarbonization in the cement industry. Existing research indicates that using industrial solid waste and other low-carbon alternative materials to partially replace traditional cement can reduce the environmental load of cementitious materials while avoiding or minimizing the high-temperature calcination process. This approach is considered one of the significant and scalable strategies for achieving near- and medium-term emission reductions in the cement industry [4–6]. Against this backdrop, the development of a new cementitious material system with high solid waste content and low cement content has become an important research direction in the field of green and low-carbon building materials, progressing toward sustainable solid waste resource recovery.

Alkali-activated materials (AAMs) and geopolymers are currently recognized as the most promising alternative technology paths to Portland cement. Since Davidovits introduced the concept of geopolymers in 1978 [7], Palomo et al. have [8] used "geopolymer" as a commercial designation linked to the alkali activation of kaolinite, limestone, and dolomite. Furthermore, Provis [9] recognized Kühl's 1908 patent as the first patent to adopt alkali activation of aluminosilicate precursors to develop substitutes for ordinary Portland cement. Since then, alkali-activated material systems using fly ash, slag, pozzolan, and other natural or industrial aluminosilicate materials as precursors have received widespread attention [10,11]. In an alkaline environment, the active Si and Al structures in the precursor undergo depolymerization, and further undergo recombination, condensation, and other reactions to form reaction products with gelling properties [7,12]. Compared with traditional Portland cement, alkali-activated materials typically exhibit higher early strength, superior resistance to high temperatures and chemical attack [13–15], and good durability under specific exposure conditions. Their durability behavior, however, is not universally established: experimental evidence concerning chloride penetration, susceptibility to efflorescence, and resistance to alkali–silica reaction remains controversial [16,17]. Li et al. [18] found that the synergistic modification of PMHS and graphene oxide enables the fly-ash-based polymer to obtain three-dimensional superhydrophobicity while maintaining mechanical strength, which can suppress moisture intrusion and improve durability. Additionally, they can make extensive use of industrial solid waste, making them a significant direction for constructing a low-carbon green cementitious material system. However, the environmental benefits of alkali-activated systems do not solely depend on a reduction in cement content. The type and dosage of activators employed, as well as the production process, also significantly impact their overall environmental footprint. Therefore, achieving high utilization of solid waste and low environmental impact while maintaining cementitious performance remains a crucial challenge to be addressed for the large-scale application of alkali-activated materials.

Biomass ash (BA) is the primary solid by-product generated during the combined heat and power generation or power generation process of biomass fuel. Depending on its generation and collection location, it can generally be classified into fly ash and bottom ash [19]. With the continuous expansion of the global renewable resource utilization scale, the development of the biomass energy industry will further increase the production of biomass ash, and the resulting demand for resource recovery and disposal is also receiving increasing attention [20]. Biomass ash typically contains abundant elements such as Si, Ca, and Al. Its mineral composition and chemical properties endow it with potential application value as a supplementary cementitious material or a precursor for alkali-activated systems [21–23], providing a promising material for solid-waste valorization in low-carbon cement systems. Existing research has shown that the chemical activity of pozzolanic materials such as biomass ash can be improved through appropriate physical or chemical pretreatment [24]. For example, Pantić et al. [25] found that mechanical grinding can sig-

nificantly increase the specific surface area of biomass ash and its reactivity as an auxiliary cementitious material; Lyu Yang et al. [26] found that introducing biomass ash into an alkali-activated cementitious system at a low mixing ratio could enhance the hydration heat release and 28-day compressive strength of the system; and Yang et al. [27] further reported in their study that when the substitution ratio of straw biomass ash does not exceed 30%, the 28-day compressive strength of composite cement can reach 42.5 MPa. Biomass ash can also be co-applied with other industrial by-products in multi-solid-waste systems. Kang et al. [28] reported that adding 15% steel slag and 9% rice husk ash significantly enhanced the compressive strength and elastic modulus of solidified high-plasticity clay and improved its microstructure. The aforementioned research indicates that biomass ash not only possesses considerable potential for resource utilization but can also effectively exhibit its cementitious activity through appropriate pretreatment and system design.

However, compared to traditional industrial by-products such as fly ash and slag, research on biomass ash as a component of alkali-activated materials is still mainly focused on low-content applications. Its potential value in cementitious systems with high solid waste content has not been fully explored. In existing research, the substitution rate of biomass ash is usually controlled within 30% [26,27], and this low utilization rate limits its large-scale consumption capacity and potential resource and environmental benefits. It is worth noting that in recent years, scholars have designed landfill ash-based hybrid alkaline cement systems with solid waste content up to 70% or even higher [29–32], and these have shown good mechanical properties and environmental benefits. These studies indicate that through rational design of the cementitious system and activation regulation, it is entirely possible to achieve a functional transformation of high-proportion solid waste from "physical filling" to "cementitious reaction." This also provides important insights for further increasing the utilization proportion of biomass ash in alkali-activated materials [33,34]. However, in high-volume biomass ash systems, changes in precursor reactivity, particle characteristics, and chemical composition may significantly affect the reaction process, workability, and mechanical properties of the system. Therefore, further research is needed to explore how to fully unleash the potential reactivity of biomass ash through appropriate pretreatment and activation strategies, and to obtain a stable cementitious system under high-volume conditions.

In addition, the low-carbon advantage of alkali-activated materials cannot be solely judged based on the cement substitution rate. Although reducing cement content can significantly decrease carbon emissions from limestone calcination and fuel consumption, the raw material preparation, energy consumption, and transportation processes of alkaline activators also generate non-negligible environmental loads, which may even offset the emission reduction benefits brought by high solid waste content to a certain extent [35]. Therefore, it is necessary to combine material performance evaluation with full life cycle environmental assessment to quantitatively evaluate the environmental performance of high-volume biomass ash-based hybrid alkaline materials from a full life cycle perspective [36], so as to more objectively assess their actual carbon reduction and energy-saving potential.

Based on this, this study utilizes fly ash (hereinafter referred to as Biomass ash-BA) generated from the Santa Maria Biomass Power Plant in Spain as the primary raw material (Lucena, Spain). The aim is to develop a high-volume biomass ash-based hybrid alkaline cement, and to systematically investigate its pretreatment, alkali activation regulation, and environmental effects. Firstly, the potential reactivity of biomass ash treated by three pretreatment methods, namely untreated, ground, and sieved, is compared. These three types of ash are mixed with cement to prepare blended cement, and its reactivity is evaluated based on the Blaine specific surface area, pozzolanic activity, and mechanical properties. Secondly, using a benchmark system of 70% biomass ash + 30% CEM I 52.5R (CB37), the

study explores the regulatory effects of four activators, namely sodium carbonate, sodium sulfate, sodium silicate, and sodium citrate, as well as their combined formulations, on the workability and mechanical properties of the composite cement system. Finally, employing the life cycle assessment method, the global warming potential (GWP) and cumulative energy demand (CED) are used as primary indicators to quantitatively evaluate the life cycle environmental load of different experimental groups. This comprehensive evaluation aims to assess the carbon emission reduction and energy-saving potential of high-volume biomass ash-based hybrid alkaline cement and advance the practical deployment of solid-waste-based low-carbon green cement.

2. Materials and Methods

2.1. Materials

2.1.1. Cement

The cement used was CEM I 52.5R ordinary Portland cement produced in Seville, Spain. Its particle size distribution and XRD pattern are shown in Figure 1a,b, respectively. The $D_v(10)$, $D_v(50)$, and $D_v(90)$ of CEM I were 1.59 µm, 9.49 µm, and 29.1 µm, respectively, indicating a broad overall distribution with marked particle-size variation. The main mineral phases include alite (C_3S), belite (C_2S), tricalcium aluminate (C_3A), tetracalcium aluminoferrite (C_4AF), and a small amount of anhydrite. Its main chemical compositions are listed in Table 1.

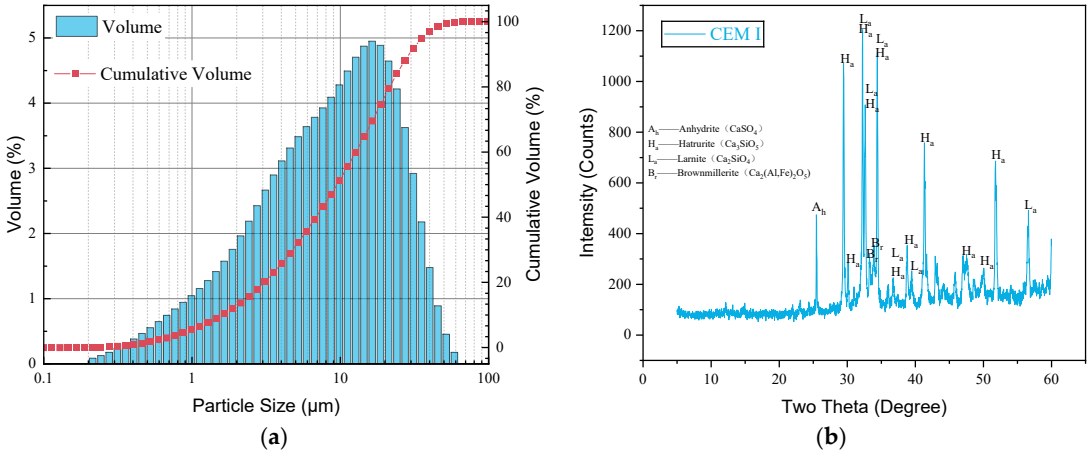


Figure 1. CEM I particle size distribution and X-ray diffraction pattern. (**a**) CEM I particle size distribution. (**b**) CEM I X-ray diffraction pattern.

Table 1. Main chemical components of CEM I 52.5R.

Raw Material/%	SiO_2	Al_2O_3	CaO	Fe_2O_3	K_2O	MgO	SO_3	Others	LOI
CEM I	18.1	3.3	61.5	3.0	0.5	3.3	3.0	2.4	4.9

2.1.2. Biomass Ash

The biomass ash was sourced from the Santa Maria Biomass Power Plant (Lucena, Spain), with an initial moisture content of 0.94%. The ash was placed in a drying oven and dried at 105 °C for 24 h to obtain original biomass ash (OBA) with a density of 2.404 g/cm^3. The dried ash was then placed in a ball mill and ground until 98 wt.% of the particles were smaller than 20 µm, resulting in ground biomass ash (GBA) with a density of 2.663 g/cm^3. The dried ash was further sieved in a negative pressure screening machine to obtain sieved biomass ash (SBA) with a density of 2.455 g/cm^3. The particle size distributions of the ashes

pretreated in the three ways are shown in Figure 2a–c. Figure 2d shows the characteristic particle sizes of OBA, GBA, and SBA. The overall particle size distribution of OBA spans a wide range, whereas the particle size of GBA is significantly finer compared to OBA, with the overall distribution shifting towards smaller particle sizes. The large particles of SBA were mostly removed, and the main particle size was concentrated around 10 μm, but the overall content of fine particles was lower than that of GBA.

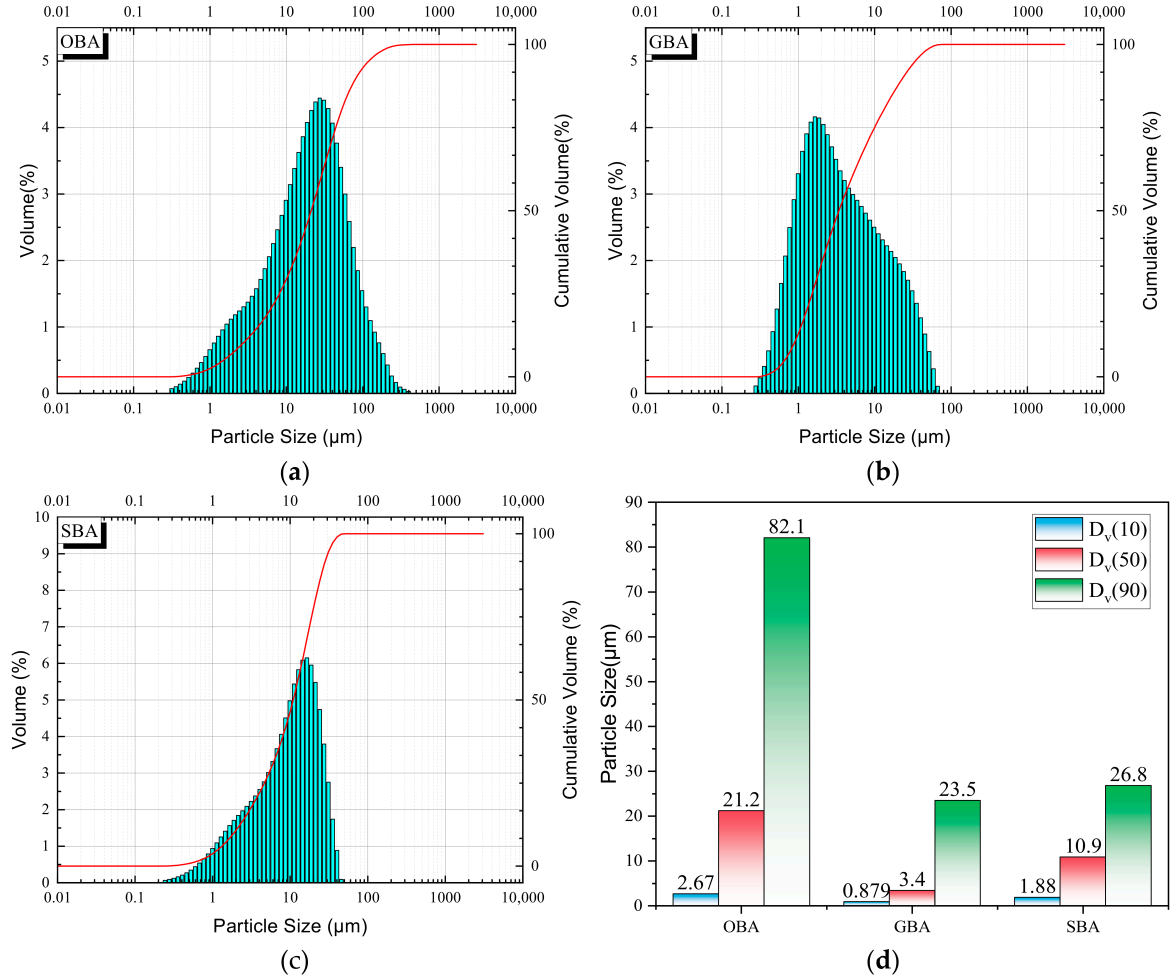


Figure 2. Particle size distribution and characteristic particle size of OBA, GBA, and SBA. (**a**) OBA particle size distribution. (**b**) GBA particle size distribution. (**c**) SBA particle size distribution. (**d**) OBA, GBA, and SBA's characteristic particle sizes.

Figure 3 presents the XRD patterns of three different pretreated biomass ashes: OBA, GBA, and SBA from bottom to top. The mineral compositions of the three ashes are similar, mainly including quartz, lime, anhydrite, albite, etc. The difference lies in the peak intensities of different phases, indicating variations in the content of mineral components. Overall, there is little difference between OBA and GBA. Notably, the albite phase in OBA is significantly higher at approximately 28°, compared to GBA and SBA. It is speculated that the crystal structure of albite was disrupted during grinding, leading to a decrease in peak intensity for GBA at this position. Meanwhile, screening removed some coarse particles rich in albite, resulting in a decrease in content and a reduced peak intensity. Additionally, it was observed that SBA exhibits more derivative peaks between 30° and 40° compared to OBA, which may be due to the enrichment of fine particles after removing coarse particles through screening.

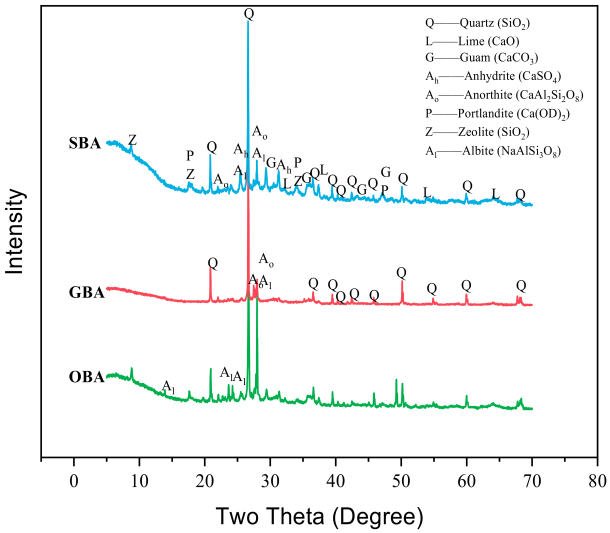


Figure 3. Mineral composition of OBA, GBA, and SBA.

The main chemical compositions of OBA, GBA, and SBA are shown in Table 2. They are primarily composed of silicates and oxides of calcium and iron, which are formed from elements such as silicon, aluminum, calcium, iron, and potassium. The loss on ignition (LOI) values are 3.9%, 4.1%, and 7.5%, respectively. The chemical composition of the three ashes is relatively similar. The SiO_2 content of GBA is higher than that of OBA and SBA, which is speculated to result from the structural damage of other products such as calcium carbonate crystals, leading to a relative increase in SiO_2 content. Conversely, the SiO_2 content of SBA is lower than that of OBA, which is speculated to be due to the removal of some coarse particles rich in SiO_2 during screening.

Table 2. Main chemical components of OBA, GBA, and SBA.

Raw Materials/%	SiO_2	Al_2O_3	CaO	Fe_2O_3	K_2O	MgO	SO_3	Others	LOI
OBA	38.5	17.9	14.5	7.9	5.7	3.1	2.0	6.5	3.9
GBA	44.8	14.2	12.4	9.0	5.9	1.9	1.2	6.5	4.1
SBA	31.9	16.4	18.6	8.0	5.3	3.2	2.5	6.6	7.5

2.1.3. Other Chemical Reagents

The chemical additives used in the activation process of Biomass Ash-based Hybrid Alkaline Cements (BHACs) include sodium sulfate, sodium carbonate, sodium silicate, and sodium citrate, with specific parameters shown in Table 3.

Table 3. Specific parameters of chemical additives.

Name	Chemical Formula	Short Name	Manufacturer	Purity or Quality Fraction
Sodium Carbonate	Na_2CO_3	Ca	Panreac (Barcelona, Spain)	99.8%
Sodium Sulfate	Na_2SO_4	Su	LabKem (Barcelona, Spain)	99%
Sodium Silicate	Na_2SiO_3	Si	IQE Group (Barcelona, Spain)	n = 1.0/3.3 (SiO_2/Na_2O)
Sodium Citrate	$Na_3C_6H_5O_7$	Ci	LabKem (Barcelona, Spain)	≥99.7%

2.2. Methods

We prepared the precursor by hand-mixing according to the mass ratio of CEM I:biomass ash = 3:7, then uniformly mixed it according to the mass ratio of precursor:chemical additive = 95:5. Finally, we ground it for 1 min at a speed of 1100 r/min using a disk grinding instrument to obtain biomass ash-based alkali-activated composite cement. The specific proportions for each experimental group are shown in Table 4. It should be noted that in preliminary experiments, it was found that excessive sodium carbonate would cause the composite cement to harden too quickly. Therefore, the same mass of grinding standard sand (BECKUM, Beckum, Germany) was added to replace an equivalent amount of sodium carbonate, keeping the total mass of the system unchanged. Each experimental group was named according to its composition and alkali activation type: C—Cement; B—Biomass ash; Ca—Sodium Carbonate, Na_2CO_3; Su—Sodium Sulfate, Na_2SO_4; Si—Sodium Silicate, Na_2SiO_3; Ci—Sodium Citrate, $Na_3C_6H_5O_7$.

Table 4. Ratio of each test group of BHACs.

Groups	CEM I (wt.%)	GBA (wt.%)	Ca (wt.%)	Su (wt.%)	Si (wt.%)	Ci (wt.%)	Sand (wt.%)
CB37	30.0	70.0	/	/	/	/	/
CB37Ca	28.5	66.5	2.5	/	/	/	2.5
CB37Su	28.5	66.5	/	5.0	/	/	/
CB37Si	28.5	66.5	/	/	5.0	/	/
CB37Ci	28.5	66.5	/	/	/	5.0	/
CB37CaSu	28.5	66.5	1.0	2.5	/	/	1.5
CB37CaSi	28.5	66.5	2.5	/	2.5	/	/
CB37SuSi	28.5	66.5	/	2.5	2.5	/	/
CB37Ca-Ci	28.5	66.5	2.0	/	/	1.0	2.0
CB37Su-Ci	28.5	66.5	/	4.0	/	1.0	/
CB37Si-Ci	28.5	66.5	/	/	4.0	1.0	/

The Blaine specific surface area test was conducted in accordance with EN 196-6:2018 [37]. It involves measuring the time it takes for air to permeate through a layer of test material with a fixed porosity under a constant pressure difference to calculate the fineness of the powder. The Blaine specific surface area is then calculated using a formula.

The Frattini test was conducted in accordance with EN 196-5:2011 [38] to evaluate the pozzolanic activity of raw materials. The test employed a mixture of CEM I: biomass ash in a ratio of 7:3 and 3:7, with a water-to-solid ratio of 5:1. After sealing, the mixture was cured in a constant-temperature oven at 40 ± 1 °C for 7 days, with two parallel samples set up for each group. After curing, the mixture was filtered, and the OH- concentration in the filtrate was titrated using a standard HCl solution (Barcelona, Spain). The CaO concentration was titrated using a standard EDTA solution (Barcelona, Spain), and compared with the saturation curve of $Ca(OH)_2$ at 40 °C.

Mortar and paste specimens for the mechanical property tests were prepared in accordance with EN 196-1:2016 [39], and prismatic specimens of 4 cm × 4 cm × 16 cm were cast. All specimens were cured under constant temperature and humidity conditions of (20 ± 2) °C and 90% relative humidity; they were demoulded 24 h after casting and curing continued until the designated test age. Flexural and compressive tests were conducted using an Ibertest Autotest 200/10 SW testing machine (Madrid, Spain), with three specimens tested per group per age for flexural strength and six specimens for compressive strength.

2.3. Life Cycle Assessment

To comprehensively evaluate the environmental sustainability of BHACs, the Life Cycle Assessment (LCA) method was employed to quantitatively assess resource consumption and environmental emissions throughout the entire process from raw material acquisition to final disposal [40]. The functional unit is set as 1 kg of cementitious material, and the system boundary adopts a "cradle-to-gate" approach, encompassing stages such as raw material production and transportation, biomass ash pretreatment, and mixing preparation. The benchmark system is CEM I 52.5R cement.

2.3.1. Life Cycle Inventory

This study adopts the zero-burden allocation hypothesis for industrial by-products [36]: biomass ash, as a by-product of the biomass power generation process, does not carry any environmental load from the production stage. This is justified because the power plant's primary function is electricity generation, to which the full plant burden is allocated; the sensitivity of this assumption to mass-based allocation is tested in Section 3.3.3 (scenario E). The CEM I 52.5R data are taken from the EPD report by Heidelberg Materials (Heidelberg, Germany) [41]. Chemical additives and electricity transportation data are taken from similar research literature and official reports [42–52]. Transportation is assumed to be by road freight, with a distance of 100 km. Electricity consumption is determined by equipment power, operation time, and grinding quality. Taking 1 kg of BHAC cementitious material as an example, its input list is shown in Table 5.

Table 5. Input list for 1 kg BHACs.

Category	Name	Unit	Number
Materials	CEM I	kg	0.285
Materials	GBA	kg	0.665
Materials	Chemical additives	kg	0.05
Energy	Electricity	kWh	0.0446
Transportation	Highway freight transport	t × km	0.1000

2.3.2. Environmental Impact Assessment

Two indicators, Global Warming Potential (GWP) and Cumulative Energy Demand (CED), are selected to evaluate the carbon emissions and energy consumption of BHACs. The calculation formulas are shown as (1) and (2).

$$GWP = \sum (A_i \times EF_i) \quad (1)$$

GWP-BHAC global warming potential, $kgCO_2eq$; A_i—activity level of the ith substance or energy source (such as electricity consumption in kWh, mass in kg, etc.); EF_i—carbon emission factor of the ith substance or energy source, with the values of carbon emission factors for each parameter shown in Table 6.

$$CED = \sum \left(A_i \times EF_{energy,i} \right) \quad (2)$$

CED-BHACs cumulative energy demand, MJ; A_i—activity level of the ith substance or energy (such as electricity consumption kWh, mass kg, etc.); $EF_{energy,i}$—primary energy demand factor of the ith input, with the primary energy demand factors for each parameter shown in Table 6.

Table 6. Environmental factors of BHAC parameters.

Parameter	Carbon Emission Factor	Unit	Primary Energy Demand Factor	Unit
CEM I	0.688 [41]	$kgCO_2eq/kg$	4.3 [41]	MJ/kg
BA	0	$kgCO_2eq/kg$	0	MJ/kg
Na_2CO_3	1.26 [42]	$kgCO_2eq/kg$	13.6 [46]	MJ/kg
Na_2SO_4	0.395 [43]	$kgCO_2eq/kg$	6.7 [47]	MJ/kg
Na_2SiO_3	1.14 [44]	$kgCO_2eq/kg$	4.6 [48]	MJ/kg
$Na_3C_6H_5O_7$	3.4 [45]	$kgCO_2eq/kg$	38.8 [45]	MJ/kg
Energy	0.258 [49]	$kgCO_2eq/kWh$	8.64 [51]	MJ/kWh
Transportation	0.116 [50]	$kgCO_2eq/(t \times km)$	2.7 [52]	$MJ/(t \times km)$

3. Results and Discussion

3.1. The Impact of Different Pretreatments on BHACs

To clarify the impact of different pretreatment methods on the physicochemical properties of biomass ash, we prepared blended cement (Blended Cement-73) by mixing CEM I 52.5R cement with OBA, GBA, and SBA in a mass ratio of 7:3, and prepared another blended cement (Blended Cement-37) by mixing them in a mass ratio of 3:7. The specific proportions are shown in Table 7. The Blaine specific surface area and pozzolanic activity of original biomass ash-based blended cement (OBC), ground biomass ash-based blended cement (GBC), and sieved biomass ash-based blended cement (SBC) were tested separately. Meanwhile, mortar mechanical properties were tested according to EN 196-1:2016. The regulation mechanism of pretreatment on biomass ash-based blended cement is revealed from multiple dimensions, including powder fineness, reactivity, and macroscopic mechanical properties. The ash sample with the best comprehensive performance is selected for the subsequent preparation of alkali-activated composite cement.

Table 7. Specific proportion of blended cement.

Blended Cement	CEM I/wt.%	OBA/wt.%	GBA/wt.%	SBA/wt.%
OBC73	70.0	30.0	/	/
OBC37	30.0	70.0	/	/
GBC73	70.0	/	30.0	/
GBC37	30.0	/	70.0	/
SBC73	70.0	/	/	30.0
SBC37	30.0	/	/	70.0

3.1.1. Blaine Specific Surface Area

Blaine specific surface area is a commonly used indicator for characterizing the fineness of cement particles, and is measured and calculated using a Blaine air permeability tester in accordance with EN 196-6:2018. The purpose of this study is to select an optimal pretreatment method, and hence only the Blaine specific surface area of ground ash-based blended cement and sieved ash-based blended cement was tested. The specific physical parameters are shown in Figure 4a.

Each type of blended cement underwent two tests, and the final Blaine specific surface area (S) was calculated as the average of the two measurements. The specific results are shown in Figure 4b. It can be observed that the overall Blaine specific surface area of sieved ash-based blended cement is larger than that of ground ash-based blended cement. The Blaine specific surface areas of SBC73 and SBC37 are 5870 cm^2/g and 8516 cm^2/g, respectively, representing an increase of 10.6% and 94.9% compared to GBC. This should

not be read as evidence of a finer particle size; the high Blaine values of the sieved-ash blends are largely an artifact of their lower true density and higher porosity, which inflate the air-permeability-derived specific surface area, and may even be related to the higher loss on ignition of SBA, although further verification is required. The Blaine specific surface area of the sieved ash-based blended cement group 37 is significantly higher than that of the other groups, exceeding the conventional testing range of the Blaine permeability method (2000~6000 cm^2/g). Therefore, the test results may have some deviations and are only for reference. It should also be noted that the high Blaine specific surface area obtained from the testing of sieved ash-based blended cement cannot be equated with high reactivity. A comprehensive judgment based on both pozzolanic reactivity tests and mechanical properties is still required, and evaluation should not solely rely on the Blaine specific surface area.

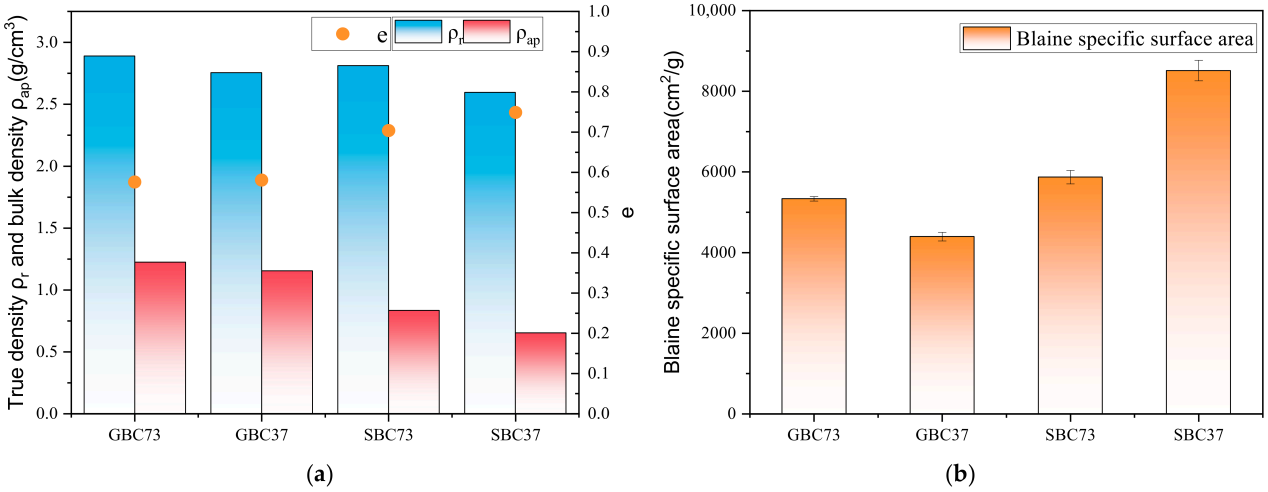


Figure 4. Blaine specific surface area of blended cement (**a**) Various physical parameters of blended cement. (**b**) Blended cement Blaine specific surface area.

3.1.2. Pozzolanic Test

To further evaluate the pozzolanic reactivity of biomass ash pretreated in different ways, the Frattini test was conducted on three types of biomass ash-based blended cements in accordance with the EN 196-5:2011. Based on the relative position of the ion concentration in the sample filtrate and the saturation solubility curve of the calcium hydroxide, the pozzolanic activity of three ash samples, namely OBA, GBA, and SBA, was evaluated.

Figure 5 shows the results of the Frattini pozzolanic activity test. The purple curve represents the solubility isotherm of $Ca(OH)_2$. Data points falling below the curve indicate that $Ca(OH)_2$ is consumed by the pozzolanic reaction, indicating that the material possesses pozzolanic activity, and the further away from the curve, the stronger the activity. From the distribution of data, the pure cement control group CEM-7d is all above the solubility curve, indicating no pozzolanic activity; in Group 73, OBC73 is above the curve, indicating no pozzolanic activity, while SBC73 and GBC73 are below the curve, proving that screening and grinding enhance the pozzolanic activity of blended cement; Group 37 is below the curve, exhibiting strong pozzolanic activity. The OH^- concentrations of OBC37, GBC37, and SBC37 are 1.82 mmol/L, 0.87 mmol/L, and 0.34 mmol/L, respectively. The difference in OH^- concentration with the same CaO concentration on the $Ca(OH)_2$ curve is 8.59 mmol/L, 9.40 mmol/L, and 8.24 mmol/L for OBC37, GBC37, and SBC37, respectively. Based on this, it can be judged that the pozzolanic activity intensity is in the order of GBC37 > OBC37 > SBC37. It should be noted that EN 196-5 was developed for pozzolanic cements with moderate clinker contents; at the 70 wt.% ash replacement used for the 37 series, the test

is applied well beyond its intended scope, and the Frattini results for the 37 series should therefore be interpreted as indicative rather than as a formal conformity assessment.

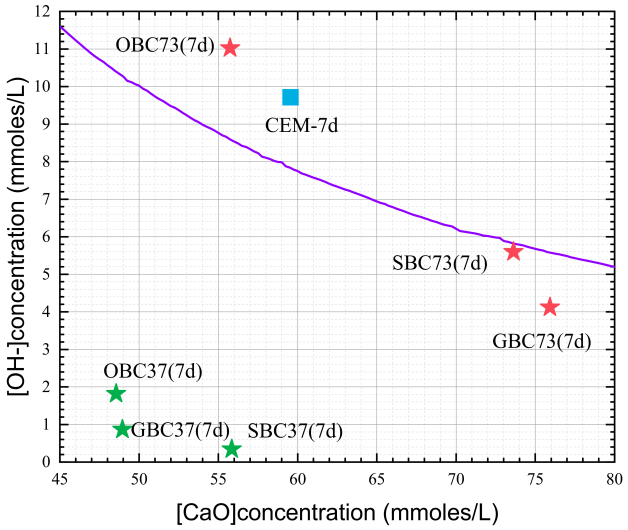


Figure 5. Pozzolanic test results. The purple curve denotes the $Ca(OH)_2$ solubility isotherm; the red and green five-pointed stars denote the 73 and 37 series blended cements, respectively; the blue square denotes the cement control (CEM-7d).

The above results indicate that high-volume biomass ash-based blended cement consumes more $Ca(OH)_2$ within the system, exhibiting stronger pozzolanic activity. Grinding has the best effect on enhancing the pozzolanic activity of blended cement, with an increase of 9.4% and 14.1% compared to raw ash and sieved ash, respectively. This is because the ball milling process not only achieves particle refinement and increases the reaction contact surface, but also destroys the inert glass shell on the surface of aluminosilicates, forming active centers on the surface and accumulating free energy reserves, thereby significantly enhancing the pozzolanic activity [53]. It is also noted that the pozzolanic activity of sieved ash-based blended cement is weaker than that of original ash-based blended cement. The SiO_2 and Al_2O_3 contents of SBA are lower than those of OBA, and the strength of pozzolanic activity is related to the contents of SiO_2 and Al_2O_3 to some extent. The decrease in these contents directly reduces the material basis for pozzolanic reaction [54], making the activity of sieved ash-based blended cement weaker than that of original ash-based blended cement.

3.1.3. Mortar Mechanical Testing

Based on the clarification of powder fineness and pozzolanic reactivity, further mechanical property tests of mortar were conducted in accordance with the EN 196-1:2016 standard to evaluate the enhancement effect of different pretreatment methods on the macroscopic properties of biomass ash-based blended cement. The water cement ratio W/B is 0.6, and the flexural and compressive strengths of three ash sample blended cements at different ages were tested. The results are shown in Figure 6.

Regarding flexural strength, the early-age (2 days) strength difference among the 73 series of biomass ash-based blended cements is relatively small, showing no significant advantage. However, at 28 days, SBC73 exhibits the best flexural strength, reaching 9.90 MPa, which is 10.2% and 10.9% higher than OBC73 and GBC73, respectively. On the other hand, the flexural strength of the 37 series of biomass ash-based blended cements is generally lower than that of the 73 series, following the pattern GBC37 > SBC37 > OBC37. GBC37 achieves a 28-day flexural strength of 7.02 MPa, which is 63.1% and 12.2% higher than OBC37 and SBC37, respectively.

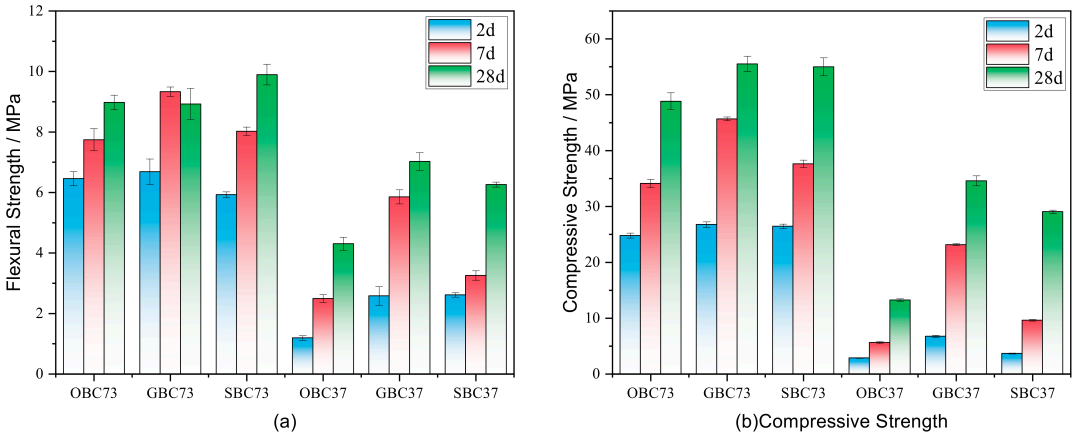


Figure 6. Strength of biomass ash-based blended cement pretreated by different methods. (**a**) Flexural strength. (**b**) Compressive strength.

Regarding compressive strength, both the 73 series and the 37 series exhibited the following pattern when cured to the same age: GBC > SBC > OBC. The early compressive strength of the 73 series was essentially the same, showing no significant strengthening effect; the 28-day compressive strengths of GBC73 and SBC73 were 55.51 MPa and 55.00 MPa, respectively, representing an increase of 13.6% and 12.5% compared to OBC73's 48.85 MPa. In the 37 series, the pretreatment effect was more pronounced: the early compressive strengths of GBC37 and SBC37 were 6.76 MPa and 3.69 MPa, respectively, representing an increase of 135.50% and 28.57% compared to OBC37's compressive strength of 2.87 MPa; the 28-day compressive strengths were 34.59 MPa and 29.06 MPa, respectively, representing an increase of 161.25% and 119.49% compared to OBC37.

Comparing the strength test results, it can be found that both grinding and screening pretreatment methods can effectively improve the strength of biomass ash-based blended cement. However, the mechanical properties of ground ash-based blended cement are superior to those of screened ash-based blended cement, especially in high-content systems. This is mainly because ball milling effectively promotes the progress of the pozzolanic reaction and the formation of gel products in the system, which macroscopically manifests as higher mechanical strength. On the other hand, screening only removes coarse particles through physical sorting, which increases the Blaine specific surface area but reduces the content of SiO_2 and Al_2O_3, limiting the pozzolanic reaction and thus the enhancement effect on strength.

Based on the combined test results of Blaine specific surface area, pozzolanic activity, and mortar mechanical properties, it can be concluded that the sieved ash from high-volume biomass ash-based blended cement exhibits the largest Blaine specific surface area, but it exceeds the conventional testing range of the Blaine permeability method and is provided for reference only. Meanwhile, the pozzolanic activity of the ground ash-based blended cement is the most pronounced, with a 28-day flexural strength of 7.02 MPa and a compressive strength of 34.59 MPa, indicating the best overall performance. Therefore, it is believed that ground ash is more suitable for high-volume biomass ash-based blended cement systems, and ground ash was selected as the solid waste precursor for subsequent alkali activation tests.

3.2. The Impact of Chemical Additives on BHACs

Based on the aforementioned pretreatment experiments, it is determined that grinding ash GBA is more suitable for the 70% high-content biomass ash blended cement system. Although mechanical pretreatment can effectively enhance the pozzolanic activity of biomass

ash, the high-content biomass ash system still faces issues of low early hydration rate and insufficient early strength development [55]. Therefore, this section focuses on the regulatory effect of chemical additives on the early mechanical properties of BHACs. BHACs are prepared using GBA as the raw material, with a fixed water-binder ratio (W/B) of 0.34. Meanwhile, the CB37 group without chemical additives is set as the control group, and the same mass of finely ground standard sand is used to replace chemical additives. The specific proportions are shown in Table 4. The evolution law of early compressive paste strength under the conditions of a single chemical additive, binary compound chemical additives, and sodium citrate compound system is studied, respectively.

3.2.1. Single Chemical Additive

To investigate the impact of four chemical additives, namely sodium carbonate, sodium sulfate, sodium silicate, and sodium citrate, on the strength of BHACs materials, a chemical additive content of 5% was designed. Considering that the exploratory tests revealed that sodium carbonate reacts too quickly with cement, leading to premature setting of the cement paste, fine-ground standard sand with a total mass of 2.5% was used to replace the corresponding mass of sodium carbonate. The specific proportions are shown in Table 4. The 2-day compressive strength was tested, and the test results are shown in Figure 7.

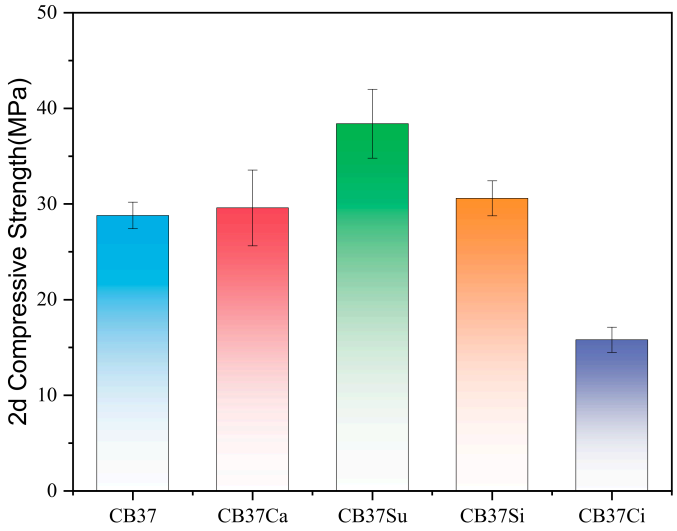


Figure 7. Early compressive strength of single chemical additive BHACs.

As shown in Figure 7, the 2 d compressive strength of the control group CB37 is 28.8 MPa, while the early compressive strengths of CB37Ca, CB37Su, and CB37Si are 29.6 MPa, 38.4 MPa, and 30.6 MPa, respectively, representing an increase of 2.8%, 33.3%, and 6.25% compared to the CB37 group. However, due to the extremely low production of early hydration products, the compressive strength of the CB37Ci group is only 15.8 MPa, which is only 54.9% of the compressive strength of the CB37 group.

Based on macroscopic observations, it is speculated that sulfate ions can react with calcium ions in the system to form ettringite, accelerating the formation of early hydration products and improving early strength, resulting in the highest compressive strength [56]. The improvement effect of sodium silicate ranks second, which may be because sodium silicate provides additional soluble silicon and promotes the formation of C-S-H gel. The improvement effect of sodium carbonate is the weakest, which may be due to its actual dosage of only 2.5%, but excessive sodium carbonate can cause premature setting. Sodium citrate acts as an organic retarder, and the citrate anions form a complex with calcium ions,

thereby inhibiting the precipitation of hydration products and significantly reducing early strength [57].

3.2.2. Dual Compound Synergistic Activation

Based on the study of a single chemical additive, this experiment further explores the synergistic activation effect of sodium carbonate, sodium sulfate, and sodium silicate at a dosage of 2.5% each. In the exploratory experiment, it was found that the reaction between sodium carbonate and sodium sulfate was too fast when combined, and the cement slurry set early. Therefore, the sodium carbonate content was reduced to 1%, and 1.5% finely ground standard sand was used instead of an equal amount of sodium carbonate. The specific ratio is shown in Table 4. The compressive strength was tested for 2 days, and the specific data is shown in Figure 8.

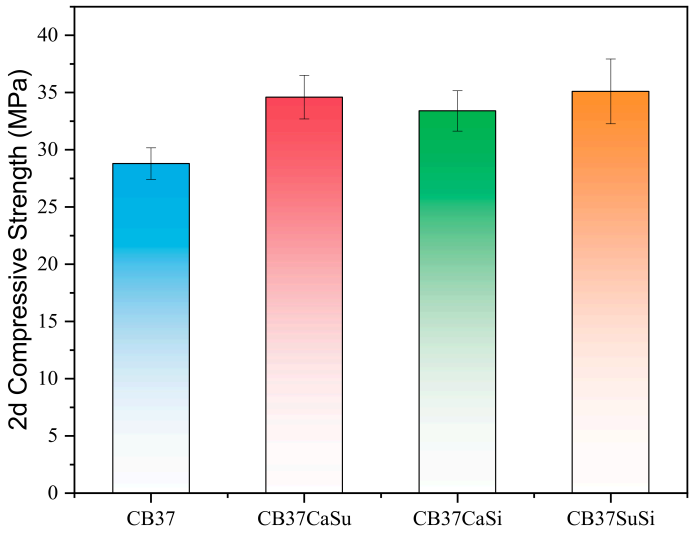


Figure 8. Early compressive strength of BHACs under binary compound chemical additives.

The compressive strengths of CB37CaSu, CB37CaSi, and CB37SuSi at 2 days were 34.6 MPa, 33.4 MPa, and 35.1 MPa, respectively, which increased by 20.1%, 16.0%, and 21.9% compared to the control group, and the increase was basically the same.

The above results indicate that the binary composite system has a certain early strength effect, higher than single sodium carbonate activation (29.6 MPa) and single sodium silicate activation (30.6 MPa), but there is no significant synergistic gain compared to single sodium sulfate activation (38.4 MPa). This phenomenon is speculated to be due to the fact that the dosage of various chemical additives in the composite system is only 2.5%, and even the concentration of sodium carbonate in CB37CaSu is only 1%, which is less than 5% of that activated by a single sodium sulfate, resulting in lower early strength than CB37Su. On the other hand, there are differences in the early promotion pathways of hydration by various chemical additives, and there may be competitive relationships and mutual interference among ions in the complex system, which cannot further accelerate the hydration process. The specific interaction mechanisms of these ions require further verification by subsequent microscopic tests.

3.2.3. Compound System of Chemical Additives and Sodium Citrate

On the basis of the above experiment, the compounding ratio of chemical additives was further adjusted by compounding sodium carbonate, sodium sulfate, and sodium silicate with sodium citrate in a ratio of 4% + 1%, respectively, to explore the synergistic activation effect of the compounding system. During the design process, it was still considered that

excessive sodium carbonate would cause the composite cement to harden too quickly. Therefore, 2% finely ground standard sand was used instead of an equal amount of sodium carbonate in the CB37Ca-Ci group. The specific ratio is shown in Table 4. The compressive strength of the test sample was tested for 2 days, and the specific data is shown in Figure 9.

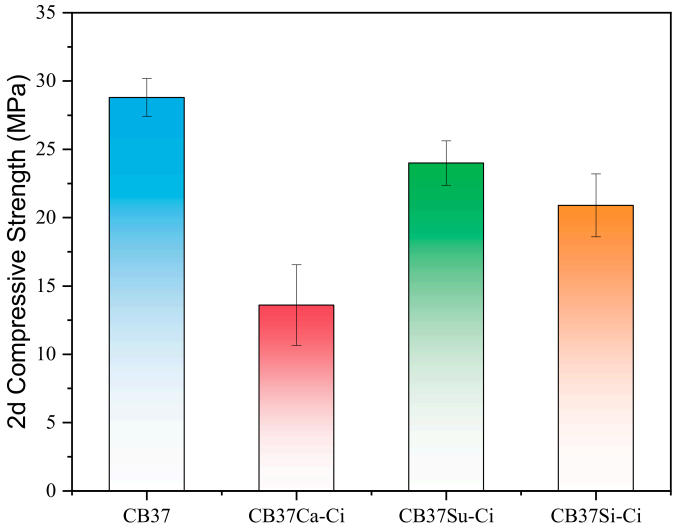


Figure 9. Early compressive strength of BHACs under the compounding of chemical additives and sodium citrate.

The compressive strengths of the CB37Ca-Ci, CB37Su-Ci, and CB37Si-Ci groups were all lower than that of the CB37 group, at 13.6 MPa, 24.0 MPa, and 20.9 MPa, respectively, which were only 47.2%, 83.3%, and 72.6% of the control group. The low early compressive strength of the combinations of chemical additives with sodium citrate may be attributed to the stronger early inhibition of hydration by sodium citrate rather than the promotion of hydration by sodium carbonate, sodium sulfate, and sodium silicate. Even with only 1% sodium citrate, its hydration inhibition exceeds the hydration-promoting effect of the other chemical additives, resulting in early strength decline. From the perspective of compressive strength, sodium citrate is not suitable as an early-strength component in this high-dosage system.

3.2.4. Synergistic Regulation of Fluidity and Early Compressive Strength

Flowability is an important indicator for characterizing the workability of alkali-activated composite cement, which is directly related to the actual engineering mixing and pouring of materials [58]. In the preliminary mechanical tests, we found that the sodium sulfate activation group had high early compressive strength, but the slurry was dry and had limited flowability. In sharp contrast, the sodium citrate activation group had extremely high slurry expansion, exceeding 130 mm, and showed obvious collapse. It can be inferred that if sodium sulfate and sodium citrate are reasonably compounded, there is potential to synergistically regulate the flowability of the slurry while ensuring mechanical properties, balancing strength and construction. To preliminarily verify this idea, this section briefly designs four experimental groups with specific ratios, as shown in Table 8. For this fluidity test series, the W/B was set to 0.5; the mix formulations and corresponding W/B ratios are summarized in Table 8. The compressive strength of each mortar sample was tested at 2 days, and the flowability of each experimental group was tested using the flow table method.

Table 8. Specific proportions for each test group in the fluidity test.

Groups	CEM I (wt.%)	GBA (wt.%)	Su (wt.%)	Ci (wt.%)	W/B
CB37Su	28.5	66.5	5	0	0.5
CB37Ci	28.5	66.5	0	5	0.5
CB37Su-Ci A	28.5	66.5	4	1	0.5
CB37Su-Ci B	28.5	66.5	4.7	0.3	0.5

Figure 10 shows the flowability and compressive strength of the experimental group at 2 days. It can be seen that the flowability of the group with only sodium sulfate is only 93.25 mm, and the slurry viscosity is high, but its early strength is relatively high, at 15.78 MPa. The flowability of the single sodium citrate group is greater than 130 mm, and the flowability of the slurry is greatly improved, but the compressive strength after 2 days is 4.24 MPa. In the complex system, the flowability of the 4% sodium sulfate complex with the 1% sodium citrate group is also greater than 130 mm, but the sodium citrate content is relatively high, and the early strength loss is significant: only 1.50 MPa. The CB37Su-Ci B group uses a combination of 4.7% sodium sulfate and 0.3% sodium citrate, with a flowability of 140.75 mm. While maintaining good flowability, the early compressive strength is the highest, reaching 17.91 MPa, achieving synergistic optimization of flowability and early mechanical properties, but the optimal ratio still needs to be systematically optimized.

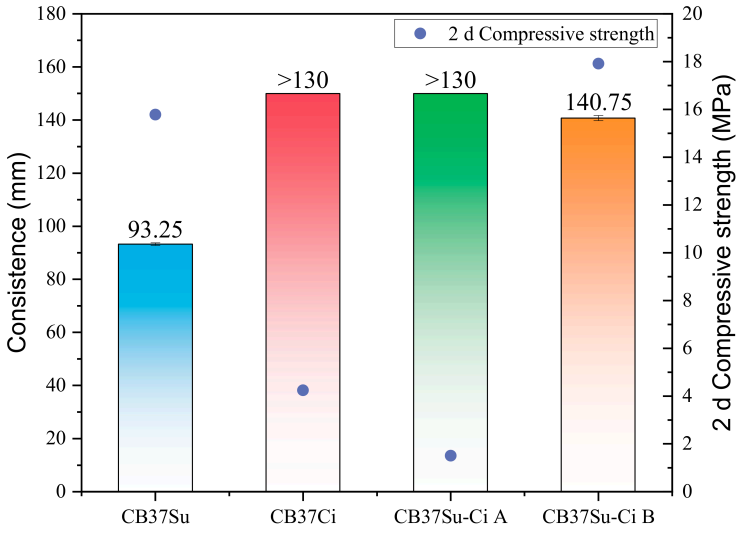


Figure 10. Flowability—2 d mortar compressive strength.

Overall, the early strength stimulation effect of single sodium sulfate is the best, with a compressive strength of 38.4 MPa at 2 days. Sodium carbonate stimulation and sodium silicate stimulation also show a slight improvement, while sodium citrate deteriorates the early strength, with a compressive strength of only 15.8 MPa at 2 days. The binary complex activation system showed early strength effects, with 2.5% sodium sulfate and 2.5% sodium silicate exhibiting the best effect, with a compressive strength of 35.1 MPa after 2 days, but no significant synergistic gain was observed. The early strength stimulation effect of the compound system of chemical additives and sodium citrate is poor, and the best effect is achieved when 4% sodium sulfate is combined with 1% sodium citrate. The compressive strength after 2 days is 24.0 MPa, which is lower than that in the control group. The synergistic regulation test of fluidity early compressive strength proves that a reasonable

sodium sulfate sodium citrate complex system can achieve significant early strength and good slurry flowability.

3.3. Comprehensive Environmental Benefit Analysis

After clarifying the effects of different pretreatment methods and chemical additives on BHACs, the GWP and CED of each experimental group of BHACs were calculated based on the above life cycle assessment method. During the calculation, the finely ground standard sand added to some experimental groups was disregarded, as it accounted for an extremely low proportion and had very low carbon emission and primary energy demand factors [59]. It should be noted that all results are based on the LCA assumption, and the specific results may vary with changes in transportation distance, regional power factors, and other parameters.

3.3.1. LCA Environmental Assessment

The calculated GWP and CED values of each BHACs group are shown in Figure 11. Owing to the 70% replacement of clinker by biomass ash, BHACs exhibit substantial carbon and energy savings relative to CEM I 52.5R; however, the type of chemical additive used can significantly alter the environmental performance of the system. Because sodium citrate has extremely high carbon emission and primary energy demand factors, the CB37Ci group exhibited the highest environmental load among all experimental groups, with a GWP of 0.389 $kgCO_2eq$ and a CED of 3.82 MJ. All citrate-free BHACs groups reduced GWP by more than 59.42% and CED by more than 45.67% relative to CEM I 52.5R. The sodium-sulfate-activated group CB37Su exhibited a GWP of only 0.239 $kgCO_2eq$, i.e., 34.74% of the reference cement, and the sodium-silicate-modified group CB37Si exhibited the lowest CED of 2.11 MJ (49.07% of the reference cement). Although grinding pretreatment and the introduction of chemical additives entail additional energy consumption and carbon emissions, this increase is smaller than the environmental benefits gained from replacing a large amount of clinker.

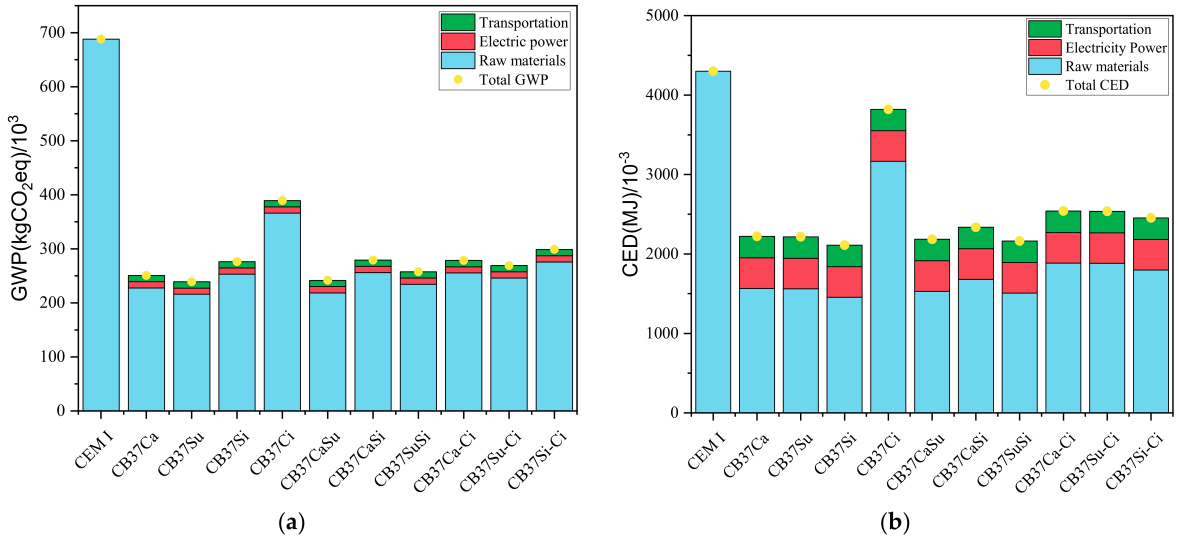


Figure 11. Environmental benefits of each BHACs test group. (**a**) GWP values of BHACs in various groups. (**b**) CED values of BHACs in various groups.

A further breakdown of the environmental loads shows that the raw material production stage is the dominant contributor for BHACs, accounting for over 90.3% of the GWP and over 68.9% of CED, while the contributions of electricity consumption and road

transportation are relatively small. This indicates that further reducing the environmental impact of BHACs should focus primarily on the selection of chemical activators, and that the potential for emission reduction through simply optimizing the grinding process or shortening transportation distances is limited.

The practical application value of materials needs to balance mechanical properties and environmental benefits. Figure 12 shows the comprehensive mechanical–environmental evaluation of each group of samples. Through comprehensive comparison, it can be seen that the CB37Su group excited by a single sodium sulfate achieved a good balance between early mechanical properties and low-carbon benefits, with a compressive strength of 38.4 MPa after 2 days, while maintaining low GWP and CED. The sodium-citrate-modified group significantly increased the environmental burden of the life cycle and deteriorated early compressive strength. However, combined with flowability testing, it was found that sodium citrate can be used to improve the flowability of the slurry, and when combined with sodium sulfate, it still has potential for application. It should be noted that the above conclusions are based only on the 2 d compressive strength and a "from cradle to gate" life cycle assessment; since durability testing has not been conducted, these conclusions are subject to certain limitations.

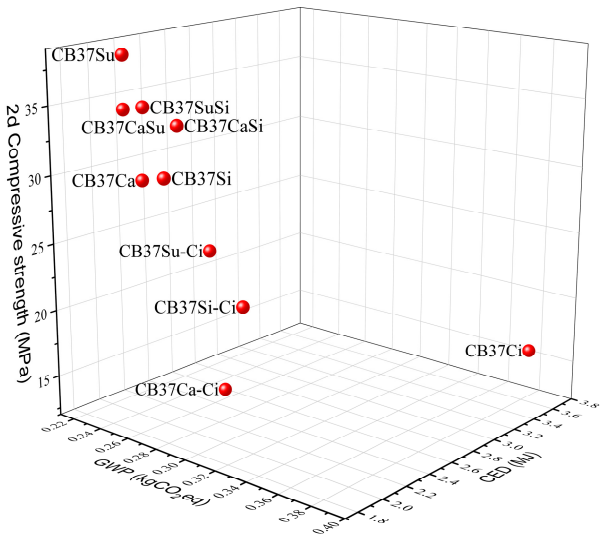


Figure 12. Mechanical environmental comprehensive evaluation.

3.3.2. Performance Normalization

The initial life cycle assessment of this study used 1 kg of dry powder cementitious material as the statistical benchmark, which only reflects the environmental load per unit mass of different cementitious systems. Since BHACs exhibit different mechanical properties under different mix ratios, a mass-based comparison alone cannot reflect their actual low-carbon potential under load-bearing conditions. Therefore, performance normalization based on the 2 d compressive strength was introduced to evaluate the environmental loads required to achieve the same compressive strength. The specific data are shown in Figure 13.

After performance normalization, the environmental loads of the experimental groups showed a similar pattern to the mass-based results: the sodium-citrate-containing groups exhibited significantly higher GWP and CED per unit strength than the citrate-free groups. The GWP and CED per MPa of the CB37Ci group reached 24.63 × 10^{-3} kgCO_2eq, and the CED reached 241.84 × 10^{-3} MJ, respectively, i.e., 3.96 and 4.19 times those of the CB37Su group. This means that, to achieve the same compressive strength, the CB37Ci group bears nearly four times the environmental load of CB37Su. The CB37Ca-Ci group also showed

high normalized GWP and CED (20.47 × 10^{-3} $kgCO_2eq$ and 186.84 × 10^{-3} MJ), mainly owing to the low 2 d compressive strength of CB37Ca-Ci (only 13.6 MPa).

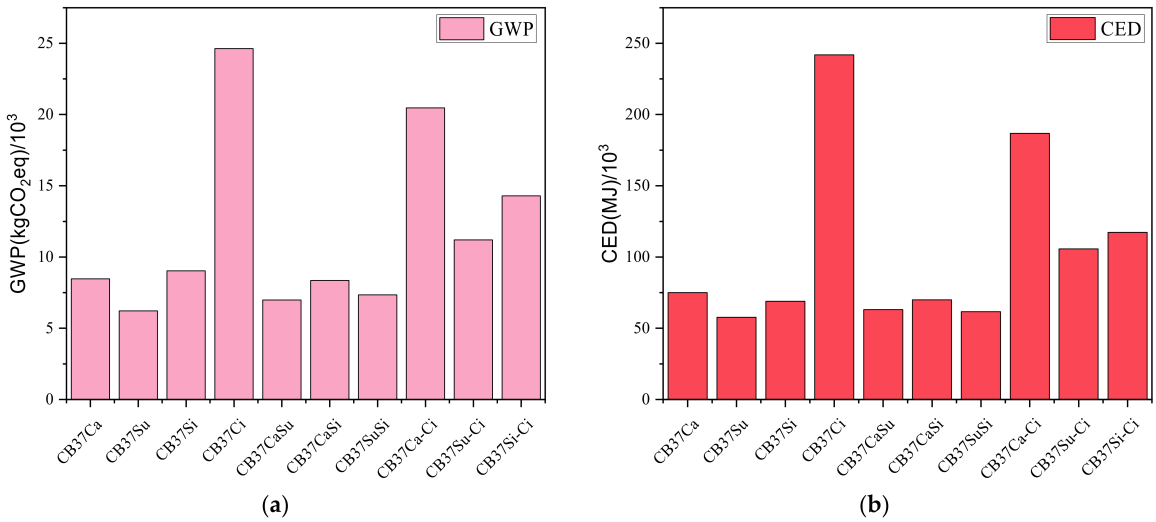


Figure 13. Normalized performance of GWP and CED. (**a**) GWP values of BHACs in each experimental group under performance normalization. (**b**) CED values of BHACs in each experimental group under performance normalization.

3.3.3. Parameter Sensitivity Analysis

The output results of LCA are constrained by input parameters and scenario assumptions. To identify the influence of key variables on the evaluation conclusions, a single-factor sensitivity analysis was conducted on CB37Su, which exhibited the best comprehensive performance. The transportation distance, regional electricity factor, activator emission factor, and biomass ash allocation approach were varied, and five scenarios were set: baseline, long-distance transportation, high power factor, high activator emission factor, and mass-based allocation. The parameter settings are shown in Table 9.

Table 9. Parameter settings of the various scenarios.

Scenario	Parameter Settings
Baseline scenario A	Zero burden of biomass ash; the transportation and power settings are shown in Table 5.
Long distance transportation scenario B	The transportation distance is set to 500 km, and the rest is the same as the baseline scenario.
High power factor scenario C	The power factor is set to 0.45 $kgCO_2eq$/kWh and 11.5 MJ/kWh, with the rest being the same as the baseline scenario.
High activator emission factor scenario D	Increase the environmental load of raw materials by 30%; other settings as in the baseline scenario.
Mass-based allocation scenario E	A share of the biomass power plant's environmental burden proportional to the mass of ash produced is allocated to the ash (allocation factor: 7%, roughly calculate by referencing relevant literature [60,61]); other settings as in the baseline scenario.

Figure 14 shows the global warming potential (GWP) and cumulative energy demand (CED) of the sodium-sulfate-activated group CB37Su under different scenarios. In all scenarios, both the GWP and CED of the BHACs increased to some extent. Compared with the baseline scenario, the GWP increased by 19.2%, 3.77%, 27.20%, and 1.31% under

scenarios B, C, D, and E, respectively, and the CED increased by 48.65%, 5.41%, 20.72%, and 8.56%, respectively. This also indirectly confirms that the raw material stage bears the main environmental load of BHACs, that transportation has a significant impact on the energy consumption of BHACs, and that mass-based allocation of the biomass power plant burden has a relatively small impact on the environment. Even under the aforementioned unfavorable conditions, the BHACs retain significant energy-saving and emission-reduction advantages, with GWP and CED reductions of over 55.81% and 23.26%, respectively, compared with traditional CEM I 52.5R cement.

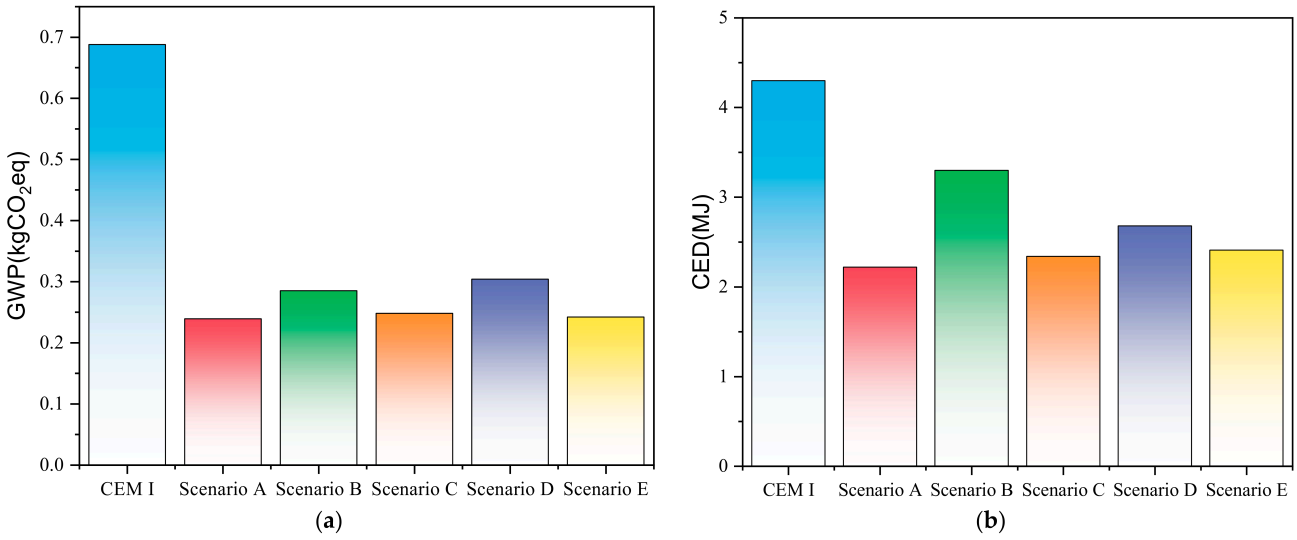


Figure 14. GWP and CED values of CB37Su under various scenarios. (**a**) GWP values of CB37Su under different scenarios. (**b**) CED values of CB37Su under different scenarios.

4. Conclusions

This article presents high-volume biomass ash-based hybrid alkaline cements (BHACs) for solid-waste valorization and the development of low-carbon green cement, and explores the effects of different pretreatment methods and four chemical additives, sodium carbonate, sodium sulfate, sodium silicate, and sodium citrate, as well as their composite systems, on BHACs' 2 d compressive strength. Conducting a "cradle–gate" life cycle assessment to quantitatively evaluate the environmental impact of BHACs, the following conclusions were drawn:

(1) The mechanical pretreatment method significantly affects the activity and performance of high-content biomass-ash-based blended cement. Screening refines the particle size and markedly increases the Blaine specific surface area; however, under high-dosage conditions, this exceeds the conventional testing range of the Blaine method and leads to a deficiency in aluminosilicate components, so the improvement in pozzolanic activity is limited. Mechanical grinding significantly improved the pozzolanic activity of the biomass ash. The ground-ash-based blended cement with a high dosage of biomass ash showed the best pozzolanic activity and mortar mechanical properties, with a 28 d compressive strength of 34.59 MPa, and is therefore suitable for high-dosage biomass-ash-based blended cement systems.

(2) Chemical additives and their combinations play a significant regulatory role in the early strength of BHACs. Single-component sodium sulfate showed the best activation performance, with a compressive strength of 38.4 MPa at 2 d, whereas sodium citrate inhibited early hydration. The binary systems exhibited no significant synergistic gain: the combination of 2.5% sodium sulfate and 2.5% sodium silicate gave the best

activation effect, with a 2 d compressive strength of 35.1 MPa, while the retarding effect of 1% sodium citrate prevailed in the citrate-containing composite systems, whose 2 d compressive strength fell below that of the control group. Flowability tests confirmed that a properly formulated sodium sulfate–sodium citrate system has potential to achieve a synergistic combination of early strength and flowability in BHACs.

(3) The high dosage of biomass ash replacing cement endows BHACs with outstanding low-carbon and energy-saving benefits, but it relies more on the selection of chemical additives. The results of the life cycle assessment indicate that the GWP of the citrate-free BHACs groups decreased by more than 59.42% relative to CEM I 52.5R, and the CED decreased by more than 45.67%. The environmental load of BHACs mainly comes from the raw material production stage, with relatively small contributions from electricity and transportation. Performance normalization based on the 2 d compressive strength further demonstrated that the CB37Ci group carries nearly four times the environmental load of the CB37Su group per unit strength, indicating that systems with weaker early strength incur substantially higher environmental burdens to deliver equivalent performance. Parameter sensitivity analysis demonstrated that the environmental advantages of BHACs are robust: even under long-distance transportation, a high-carbon electricity mix, increased raw-material burdens, and mass-based allocation of the biomass power plant burden, CB37Su retained GWP and CED reductions of over 55.81% and 23.26%, respectively, relative to CEM I 52.5R.

Therefore, on the basis of 2-day compressive strength data and cradle-to-gate life cycle assessment results, BHACs exhibit considerable potential for reconciling mechanical performance with environmental benefits, enabling high-value valorization of solid waste and promoting technological innovation in green low-carbon cement development.

Author Contributions: Conceptualization, L.X.; methodology, L.X. and X.C.; validation, L.X. and X.C.; formal analysis, X.C. and L.X.; investigation, L.X., X.C., O.M., Z.W. and A.P.; resources, L.X., Z.W., O.M. and A.P.; data curation, L.X. and X.C.; writing—original draft preparation, L.X. and X.C.; writing—review and editing, L.X., X.C., O.M., Z.W. and A.P.; visualization, L.X. and X.C.; supervision, L.X., Z.W. and A.P.; project administration, L.X.; funding acquisition, L.X. All authors have read and agreed to the published version of the manuscript.

Funding: This research was funded by the National Natural Science Foundation of China (Grant No. 52604216), the China Postdoctoral Science Foundation (Project No.: 2024M763561) and the Fundamental Research Funds for the Central Universities (Project No.: 2025QN1015).

Institutional Review Board Statement: Not applicable.

Informed Consent Statement: Not applicable.

Data Availability Statement: The original contributions presented in this study are included in the article. The datasets, processed results and analysis code will be made available upon reasonable request; further inquiries can be directed to the corresponding author.

Conflicts of Interest: The authors declare no conflicts of interest.

Abbreviations

The following abbreviations are used in this manuscript:

BHACs	Biomass Ash-based Hybrid Alkaline Cements
BA	Biomass Ash
OBA	Original Biomass Ash
GBA	Ground Biomass Ash
SBA	Sieved Biomass Ash
OBC	Original Biomass Ash-based Blended Cement

GBC	Ground Biomass Ash-based Blended Cement
SBC	Sieved Biomass Ash-based Blended Cement
LCA	Life Cycle Assessment
GWP	Global Warming Potential
CED	Cumulative Energy Demand
Ca	Sodium Carbonate
Su	Sodium Sulfate
Si	Sodium Silicate
Ci	Sodium Citrate

References

1. Sverdrup, H.U.; Olafsdottir, A.H. Dynamical modelling of the global cement production and supply system, assessing climate impacts of different future scenarios. *Water Air Soil Pollut*. **2023**, *234*, 191. [CrossRef]
2. Dmitrieva, E.; Potapova, E. Effect of heat-treated polymineral clays on the properties of portland cement paste. *Mater. Today Proc*. **2021**, *38*, 1663–1668. [CrossRef]
3. Andrew, R.M. Global CO 2 emissions from cement production, 1928–2018. *Earth Syst. Sci. Data* **2019**, *11*, 1675–1710. [CrossRef]
4. Environment, U.; Scrivener, K.L.; John, V.M.; Gartner, E.M. Eco-efficient cements: Potential economically viable solutions for a low-CO2 cement-based materials industry. *Cem. Concr. Res*. **2018**, *114*, 2–26. [CrossRef]
5. Habert, G.; Miller, S.A.; John, V.M.; Provis, J.L.; Favier, A.; Horvath, A.; Scrivener, K.L. Environmental impacts and decarbonization strategies in the cement and concrete industries. *Nat. Rev. Earth Environ*. **2020**, *1*, 559–573. [CrossRef]
6. Barbhuiya, S.; Bhusan Das, B.; Adak, D. Roadmap to a net-zero carbon cement sector: Strategies, innovations and policy imperatives. *J. Environ. Manag*. **2024**, *359*, 121052. [CrossRef]
7. Davidovits, J. Geopolymers. *J. Therm. Anal*. **1991**, *37*, 1633–1656. [CrossRef]
8. Palomo, A.; Kryvenko, P.; García-Lodeiro, I.; Kavalerova, E.; Maltseva, O.; Fernández-Jiménez, A. A review on alkaline activation: New analytical perspectives. *Mater. Constr*. **2014**, *64*, e022. [CrossRef]
9. Provis, J.L. Geopolymers and other alkali activated materials: Why, how, and what? *Mater. Struct*. **2014**, *47*, 11–25. [CrossRef]
10. Farooq, F.; Xin, J.; Javed, M.F.; Akbar, A.; Shah, M.I.; Aslam, F.; Alyousef, R. Geopolymer concrete as sustainable material: A state of the art review. *Constr. Build. Mater*. **2021**, *306*, 124762. [CrossRef]
11. Zhang, B.; Zhu, H.; Feng, P.; Zhang, P. A review on shrinkage-reducing methods and mechanisms of alkali-activated/geopolymer systems: Effects of chemical additives. *J. Build. Eng*. **2022**, *49*, 104056. [CrossRef]
12. Provis, J.; Bernal, S. Geopolymers and Related Alkali-Activated Materials. *Annu. Rev. Mater. Res*. **2014**, *44*, 299–327. [CrossRef]
13. Singh, N.B.; Middendorf, B. Geopolymers as an alternative to Portland cement: An overview. *Constr. Build. Mater*. **2020**, *237*, 117455. [CrossRef]
14. Xiaowei, X.; Yaxiong, X.; Baifa, Z.; Guohui, L.; Siwen, Y. Recent Progress on Reaction Mechanism, Properties, and Application of Alkali-Activated Geopolymer. *Multipurp. Util. Miner. Resour*. **2023**, *44*, 83–90. (In Chinese)
15. Gökçe, H.S. Durability of slag-based alkali-activated materials: A critical review. *J. Aust. Ceram. Soc*. **2024**, *60*, 885–903. [CrossRef]
16. Pacheco-Torgal, F.; Abdollahnejad, Z.; Camões, A.F.; Jamshidi, M.; Ding, Y. Durability of alkali-activated binders: A clear advantage over Portland cement or an unproven issue? *Constr. Build. Mater*. **2012**, *30*, 400–405. [CrossRef]
17. Zhang, J.; Shi, C.; Zhang, Z.; Ou, Z. Durability of alkali-activated materials in aggressive environments: A review on recent studies. *Constr. Build. Mater*. **2017**, *152*, 598–613. [CrossRef]
18. Li, Y.; Zhong, Z.; Ma, X.; Gan, Y.; Kang, X. High-performance superhydrophobic fly ash based geopolymers with graphene oxide reinforcement for enhanced durability and repellency. *Constr. Build. Mater*. **2024**, *452*, 138944. [CrossRef]
19. Bülbül, F.; Courard, L. Turning waste into greener cementitious Building material: Treatment methods for biomass Ashes—A review. *Materials* **2025**, *18*, 834. [CrossRef] [PubMed]
20. Maj, I.; Niesporek, K.; Płaza, P.; Maier, J.; Łój, P. Biomass ash: A review of chemical compositions and management trends. *Sustainability* **2025**, *17*, 4925. [CrossRef]
21. Park, C.; Lee, J. Transforming biowaste into sustainable supplementary cementitious materials. *J. Build. Eng*. **2024**, *98*, 110976. [CrossRef]
22. Overmann, S.; Allwicher, I.; Montag, D.; Vollpracht, A.; Matschei, T. Comparative Evaluation of Different Biomass Ashes as Supplementary Cementitious Materials: Reactivity, Hydration Impact and Environmental Considerations. *Materials* **2025**, *18*, 4239. [CrossRef] [PubMed]
23. Biswas, D.; Mondal, A.; Shiuly, A.; Mondal, A.; Sau, D.; Acharya, S.; Modak, R.; Kumar, V.; Hembram, S.; Gupta, B. A review on agricultural waste ashes as sustainable supplementary cementitious materials for concrete applications. *Discov. Concr. Cem*. **2026**, *2*, 25. [CrossRef]

24. Xiong, L.; Maltseva, O.; Fernández-Jiménez, A.; Wan, Z.; Palomo, A. Mechanism for activity variation of landfilled coal ash: Deterioration in landfilling and improvement in pretreatment. *Case Stud. Constr. Mater.* **2025**, *22*, e04817. [CrossRef]
25. Pantić, V.; Šupić, S.; Vučinić-Vasić, M.; Nemeš, T.; Malešev, M.; Lukić, I.; Radonjanin, V. Effects of grinding methods and water-to-binder ratio on the properties of cement mortars blended with biomass ash and ceramic powder. *Materials* **2023**, *16*, 2443. [CrossRef] [PubMed]
26. Lv, Y.; Ge, Y.; Zhao, B.; Chen, Y.; Dan, J.; Zhou, Y.; Ke, K.; Li, X. Effect of Biomass Ash on Properties of Alkali-Activated Slag Cementitious Materials. *Bull. Chin. Ceram. Soc.* **2025**, *44*, 1288–1296. (In Chinese)
27. Yang, L.; Xu, W.Y.; Ji, Y.C.; Liu, X.; Li, C.; Wu, Y.X. Research on the properties and mechanisms of activated straw biomass ash composite cement from multiple-angle approach. *Constr. Build. Mater.* **2025**, *480*, 141500. [CrossRef]
28. Kang, X.; Li, C.; Zhang, M.; Yu, X.; Chen, Y. Mechanical properties and stabilization mechanism of steel slag-rice husk ash solidified high plasticity clay. *Geotech. Test. J.* **2024**, *47*, 235–253. [CrossRef]
29. Xiong, L.; Maltseva, O.; Chen, B.; Fernández-Jiménez, A.; Wan, Z.; Palomo, A. Modelling the hydration of ultra-low clinker cements: The impact of sodium salts additives. *Constr. Build. Mater.* **2025**, *504*, 144655. [CrossRef]
30. Xiong, L.; Maltseva, O.; Fernandez-Jimenez, A.; Wan, Z.; Palomo, A. Transforming landfilled coal ash in ultralow clinker binders. *J. Am. Ceram. Soc.* **2025**, *108*, e20661. [CrossRef]
31. Xiong, L.; Wang, L.; Wan, Z.; Chen, B.; Chang, L.; Fernández-Jiménez, A.; Palomo, A. Hydration mechanism of landfilled coal ash-based low-clinker cement and exploration of its functional application in coal mines. *J. China Coal Soc.* **2026**, *51*, 2466–2487. (In Chinese)
32. Xiong, L.; Zhang, Z.; Wan, Z.; Zhang, Y.; Wang, Z.; Lv, J. Optimization of grouting material mixture ratio based on multi-objective optimization and multi-attribute decision-making. *Sustainability* **2021**, *14*, 399. [CrossRef]
33. Krivenko, P.; Kovalchuk, O.; Pasko, A.; Croymans, T.; Hult, M.; Lutter, G.; Vandevenne, N.; Schreurs, S.; Schroeyers, W. Development of alkali activated cements and concrete mixture design with high volumes of red mud. *Constr. Build. Mater.* **2017**, *151*, 819–826. [CrossRef]
34. Li, Y.; Liu, Y.; Li, L.; Yang, S.; Kang, X. Low-carbon alkali activation of high-volume lithium slag in ternary cementitious systems: Synergistic hydration, microstructural evolution, and environmental assessment. *Sustain. Mater. Technol.* **2026**, *49*, e02191. [CrossRef]
35. Fernando, S.; Gunasekara, C.; Law, D.W.; Nasvi, M.; Setunge, S.; Dissanayake, R.; Robert, D. Environmental evaluation and economic analysis of fly ash-rice husk ash blended alkali-activated bricks. *Environ. Impact Assess. Rev.* **2022**, *95*, 106784. [CrossRef]
36. Nikravan, M.; Firdous, R.; Stephan, D. Life cycle assessment of alkali-activated materials: A systematic literature review. *Low-Carbon Mater. Green Constr.* **2023**, *1*, 13. [CrossRef]
37. *EN196-6:2018*; Methods of Testing Cement-Part 6: Determination of Fineness. European Committee for Standardization: Brussels, Belgium, 2018.
38. *EN196-5:2011*; Methods of Testing Cement-Part 5: Pozzolanicity Test for Pozzolanic Cement. European Committee for Standardization: Brussels, Belgium, 2011.
39. *EN196-1:2016*; Methods of Testing Cement-Part 1: Determination of Strength. European Committee for Standardization: Brussels, Belgium, 2016.
40. Curran, M.A. Life Cycle Assessment: A review of the methodology and its application to sustainability. *Curr. Opin. Chem. Eng.* **2013**, *2*, 273–277. [CrossRef]
41. Heidelberg Materials Hispania Cementos S.A. Declaración Ambiental de Producto: CEM I 52,5 R, Fábrica de Añorga [R]. Stockholm. 2024. Available online: https://materiales.gbce.es/wp-content/uploads/2025/08/0015650_CEM-I-52.5-R-Anorga.pdf (accessed on 26 August 2026).
42. Ausfuhrkontrolle B f W u. Informationsblatt CO2-Faktoren (Version v3.3) [R]. 2025. Available online: https://www.bafa.de/SharedDocs/Downloads/DE/Energie/eew_infoblatt_co2_faktoren_2025.html (accessed on 26 August 2026).
43. Zhou, W.; Wang, J. Research on Carbon Footprint of Anhydrous Sodium Sulfate Products Based on Life Cycle Assessment. *Mod. Chem. Res.* **2026**, 115–117. (In Chinese)
44. Lazorenko, G.; Kravchenko, E.; Kasprzhitskii, A.; Fini, E.H. An evaluation of the environmental impact and energy efficiency of producing geopolymer mortar with plastic aggregates. *Resour. Conserv. Recycl. Adv.* **2024**, *22*, 200216. [CrossRef]
45. Pati, P.; McGinnis, S.; Vikesland, P.J. Life cycle assessment of "green" nanoparticle synthesis methods. *Environ. Eng. Sci.* **2014**, *31*, 410–420. [CrossRef]
46. Simoni, M.; Hanein, T.; Woo, C.L.; Nyberg, M.; Tyrer, M.; Provis, J.L.; Kinoshita, H. Synthesis of Ca (OH) 2 and Na2CO3 through anion exchange between CaCO3 and NaOH: Effect of reaction temperature. *RSC Adv.* **2022**, *12*, 32070–32081. [CrossRef] [PubMed]

47. El Kassar, R.; Al Takash, A.; El Rassy, E.; Hammoud, M.; Py, X. Comparative Life Cycle Assessment of Inorganic and Organic PCM-Based Thermal Management in Photovoltaic Systems: A Case Study in Lebanon. In *Proceedings of the 2025 IEEE 19th International Conference on Compatibility, Power Electronics and Power Engineering (CPE-POWERENG)*; IEEE: New York, NY, USA, 2025.
48. Manhanpally, N.; Nagarajan, P.; Saha, S.; Thomas, B.S. Influence of untreated and treated recycled coarse aggregates on engineering properties of slag dolomite geopolymer concrete. *Sci. Rep.* **2025**, *15*, 26649. [CrossRef] [PubMed]
49. Climàtic O C d C. Electricity Emission Factor [Z]. 2025. Available online: https://canviclimatic.gencat.cat/en/actua/factors_demissio_associats_a_lenergia/index.html (accessed on 27 August 2026).
50. Climatiq. Rigid Truck 26-32t—Average/Mixed Load—Diesel[EB/OL]. GLEC v3.0 [Z]. 2023. Available online: https://www.climatiq.io/data/emission-factor/dcbeb133-c03f-495c-b590-fae3c4711949 (accessed on 26 August 2026).
51. Energética, E. Consulta Pública Sobre la Revisión del Cálculo de Energía Primaria de la Electricidad en Edificios [Z]. 2026. Available online: https://www.eseficiencia.es/2026/05/13/consulta-publica-revision-calculo-energia-primaria-electricidad-edificios (accessed on 27 August 2026).
52. Hosseini, S.A.; Asghari, V.; Liu, X.; Hsu, S.-C.; Poon, C.-S. Cross-country life cycle assessment of construction and demolition waste recycling with evaluation of energy use, carbon emissions, and regional trade-offs. *Sci. Rep.* **2025**, *15*, 41377. [CrossRef] [PubMed]
53. Niyazbekova, R.; Ibrayeva, Z.; Cieslik, J.; Ibzhanova, A.; Aldabergenova, S.; Serekpayeva, M. Energy-Efficient Mechanochemical Activation of Coal Fly Ash and Slag for Sustainable Cementitious Composites. *Preprints* **2026**. [CrossRef]
54. Nicoara, A.I.; Stoica, A.E.; Vrabec, M.; Šmuc Rogan, N.; Sturm, S.; Ow-Yang, C.; Gulgun, M.A.; Bundur, Z.B.; Ciuca, I.; Vasile, B.S. End-of-life materials used as supplementary cementitious materials in the concrete industry. *Materials* **2020**, *13*, 1954. [CrossRef] [PubMed]
55. Vaičienė, M.; Malaiškienė, J. Influence of biofuel bottom ash and chemical additives on hydration and physical, mechanical properties of cementitious materials. *Constr. Build. Mater.* **2026**, *531*, 146692. [CrossRef]
56. Etcheverry, J.M.; Villagran-Zaccardi, Y.A.; Van den Heede, P.; Hallet, V.; De Belie, N. Effect of sodium sulfate activation on the early age behaviour and microstructure development of hybrid cementitious systems containing Portland cement, and blast furnace slag. *Cem. Concr. Compos.* **2023**, *141*, 105101. [CrossRef]
57. Liu, Y.; Zhang, Z.; Jing, R.; Yan, P. The interaction of sodium citrate and polycarboxylate-based superplasticizer on the rheological properties and viscoelasticity of cement-based materials. *Constr. Build. Mater.* **2021**, *293*, 123466. [CrossRef]
58. Puertas, F.; Varga, C.; Alonso, M.M. Rheology of alkali-activated slag pastes. Effect of the nature and concentration of the activating solution. *Cem. Concr. Compos.* **2014**, *53*, 279–288. [CrossRef]
59. Bąk, A.; Mikuła, J.; Oliinyk, I.; Łach, M. Basic research on layered geopolymer composites with insulating materials of natural origin. *Sci. Rep.* **2024**, *14*, 12576. [CrossRef] [PubMed]
60. Zhai, J.; Burke, I.T.; Stewart, D.I. Potential reuse options for biomass combustion ash as affected by the persistent organic pollutants (POPs) content. *J. Hazard. Mater. Adv.* **2022**, *5*, 100038. [CrossRef]
61. Reaño, R.L.; de Padua, V.A.N.; Halog, A.B. Energy efficiency and life cycle assessment with system dynamics of electricity production from rice straw using a combined gasification and internal combustion engine. *Energies* **2021**, *14*, 4942. [CrossRef]

Disclaimer/Publisher's Note: The statements, opinions and data contained in all publications are solely those of the individual author(s) and contributor(s) and not of MDPI and/or the editor(s). MDPI and/or the editor(s) disclaim responsibility for any injury to people or property resulting from any ideas, methods, instructions or products referred to in the content.